PROCEEDINGS OF SCIENCE

The dynamic range of the AugerPrime Surface Detector: technical solution and physics reach

Antonella Castellina[*a] **for the Pierre Auger Collaboration**[b]
[a] *Osservatorio Astrofisico di Torino (INAF) and INFN, Sezione di Torino, Italy*
[b] *Observatorio Pierre Auger, Av. San Martín Norte 304, 5613 Malargüe, Argentina*
E-mail: auger_spokespersons@fnal.gov
Full author list: http://www.auger.org/archive/authors_icrc_2017.html

Ground arrays for ultra-high energy cosmic ray detection based on water-Cherenkov stations or scintillator modules are unavoidably limited by the saturation suffered by the counters closest to the shower axis. Reducing to a negligible level the amount of events with saturated detectors is mandatory to unambiguously record the highest energy events and to decrease the systematic uncertainties affecting the measurements. The Surface Detector Array of the upgraded Pierre Auger Observatory includes 1660 water-Cherenkov stations covered by a 3.8 m^2 plastic scintillator plane. The impact point of the extensive air shower, its arrival direction and the lateral distribution of particles at the ground can be reconstructed exploiting the recorded signals and their timing. The stations will use new electronics that will process signals from both the tanks and the scintillators with increased quality. The addition of an extra small photomultiplier in each surface station and suitable photomultipliers with very large linearity in the scintillator detectors will allow us to extend the dynamic range to more than 32 times the largest signals currently measured. We describe the chosen technical solutions and discuss the expected performance of the detectors, which will be able to measure non-saturated traces as close as a couple of hundred meters to the shower core.

35th International Cosmic Ray Conference — ICRC2017
10–20 July, 2017
Bexco, Busan, Korea

*Speaker.

PoS(ICRC2017)397

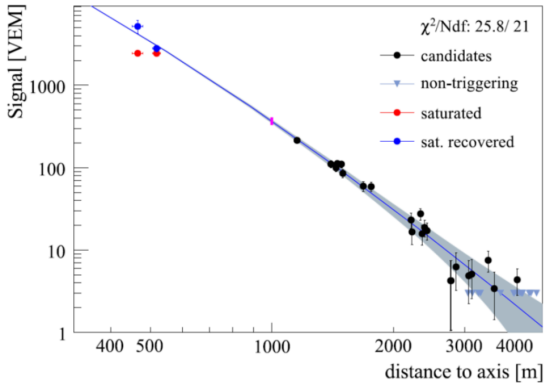

Figure 1: Lateral distribution of the signal sizes recorded in the WCD. Red circles: saturated stations. Blue circles: recovered signals.

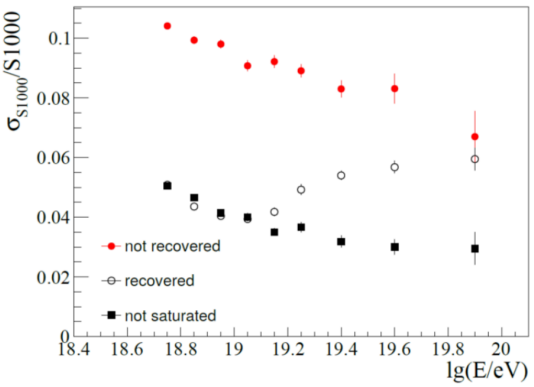

Figure 2: $S(1000)$ resolution for events without (black) or with at least one saturated station (red) and using the recovery procedure (empty).

1. Introduction

Extensive air showers with energies above 3 EeV are measured in the Pierre Auger Observatory Surface Detectors (SD) by recording the signals and arrival times of the secondary particles reaching the ground, which spread over a large area of more than 15 km^2.

The Cherenkov light produced by the secondary particles in each water-Cherenkov detector (WCD) is collected by three large 9 inch photomultipliers (Photonis XP1805), from now on LPMTs, which are individually sampled and digitized by FADC in two overlapping ranges with different resolutions. The dynamic range of the measurement varies from few photoelectrons in the stations very far from the shower core and from the low energy muon signals used to calibrate the detectors, to hundreds of thousands in the station closer to the core. When the impact point of the shower at the ground is close to a detector, the dynamic range of the recording electronics is smaller than required to record the Cherenkov signal produced by the particles. The largest particle density measurable before signal saturation is not only constrained by the acquisition electronics (e.g. anode FADC overflow) but, more substantially, by the limited extension of the LPMTs linear range, which deviates from linearity for peak currents in excess of ∼50 mA. Conservatively assuming a maximum current of 40 mA, this value is well matched via standard 50 Ω termination resistors by the 2 V input range of the front-end digitizers. A recovery procedure is currently implemented to estimate the signal in case of saturation [1], thus allowing to include the saturated stations in the lateral distribution function fits with consequent improvements in energy estimation.

An example of the lateral distribution of an event produced by a vertical 100 EeV proton is illustrated in Fig. 1 where the signal size is expressed in VEM (Vertical Equivalent Muon, i.e. the average signal from a vertical muon crossing the WCD).

Both the saturated signals and the recovered ones are shown for the stations closest to the shower core. Due to the current limited information, the accuracy of the recovered signals larger than 10^4 VEM can be worse than 70%. An accuracy as good as 15% in the measured signals can only be obtained with a detailed knowledge of the individual PMT responses in the non-linear region (a non feasible solution, which needs a measurement of the deep saturation curve of each

of the 5000 PMTs and the monitoring of their properties in time). It is important to note that the expectation value of the SD energy estimator $S(1000)$ is not affected by having a station with a saturated signal in the event, only the reconstruction resolution is worsened to some extent. The resolution in the reconstructed $S(1000)$ is related to the uncertainty in the knowledge of the lateral distribution function. Due to the choice of a specific lateral distribution function, a systematic uncertainty of less 4% is induced on $S(1000)$, at $10^{19.5}$ eV, for events without saturated stations. On the contrary, as shown in Fig. 2, this value increases to 8% if one of the signals is saturated and only a limited correction to $\sim$6% can be obtained by applying the recovery procedure.

2. The AugerPrime extended dynamic range

A substantial upgrade of the Pierre Auger Observatory (AugerPrime) [2] is underway with the main goal of improving the mass determination of primary cosmic rays in the suppression region, above $10^{19.5}$ eV. For this purpose, all the water-Cherenkov detectors of the existing surface array are equipped by a 3.8 m^2, 1 cm thick scintillator plane. Owing to their different response to the muonic and electromagnetic components of the extensive air showers, these new detectors will provide a complementary measurement of the shower particles at the ground.

The surface detector electronics has been redesigned with faster sampling ADC channels, powerful FPGA, and better timing accuracy [3] to enhance the local trigger and processing capabilities and to allow the acquisition of both water-Cherenkov and scintillator detector signals.

In particular, the SD data quality will be improved by extending the acquisition dynamic range in both detectors, thus allowing to measure non-saturated signals at distances as close as 250 m from the shower core. In order to benefit the most from the combined information of the SSD and the WCD signals, the dynamic range of both detectors should be similar. Significant signals are expected close to the shower core and also at intermediate distances, where the simultaneous measurements will be most important for the separation of the different components of the shower, furthermore allowing a direct cross-check of the two detectors.

An engineering array of 12 stations, fully equipped with scintillators and new electronics has been deployed in the field and has been taking data since October 2016.

2.1 Extended dynamic range of the water-Cherenkov detectors

When exposed to the same photon density, photomultipliers with photocathode of different size (operated at the same gain) will produce output signals proportional to their sensitive surfaces. Similarly, the introduction of an additional photomultiplier with small diameter in each surface detector can largely reduce the occurrence of saturated signal in the stations closest to the shower axis. This solution increases the linear operative range of the water-Cherenkov Detectors with limited changes to the station mechanics and electronics and without interfering with their standard operation. The small photomultiplier (hereafter SPMT) can be easily installed in the station by exploiting an unused and easily accessible 30 mm diameter window on the Tyvec bag containing the hyper-pure water of the surface detectors, avoiding any changes on the tank mechanical structure.

Different photomultipliers from various companies have been considered and tested. The final choice of the Hamamatsu-R8619 photomultiplier was the best compromise between performance

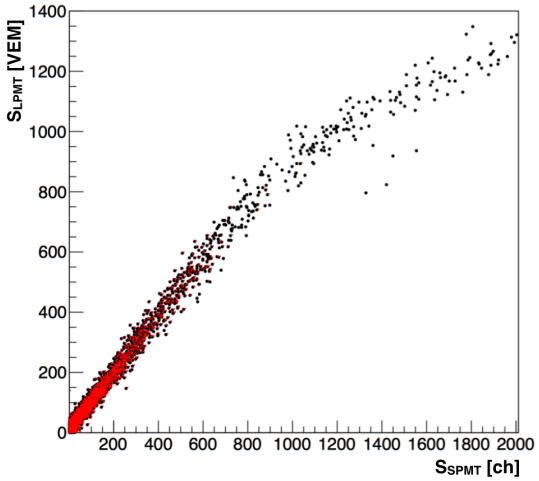

Figure 3: Average integrated signal from the 3 LPMTs (VEM) versus the SPMT signal (ADC ch). In red, the region with non-saturated LPMTs.

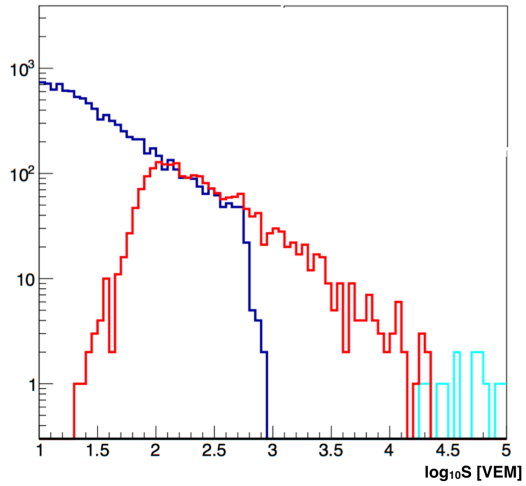

Figure 4: Logarithm of the charge for a single station, as measured by the LPMTs (blue) and by the SPMT (red and cyan).

and price. Its active area is only 1/100 of the XP1850 (LPMT), potentially allowing for an equivalent dynamic range extension. Adjusting the gain, the ratio $R = \langle S_{\rm LPMT}\rangle / S_{\rm SPMT}$ can be limited to a value of 32, enough to allow for a linear range extension of the dynamic range up to 2×10^4 VEM. The optimal R value is initially setup for each SPMT by a preliminary and fast procedure exploiting intense light pulses by the LED onboard each station. This setting almost completely eliminates the occurrence of saturated signals also at the highest energy.

The SPMT anode signal is read and digitised by the new AugerPrime electronics with a dedicated input, analogous to those for the LPMTs at lower resolution. Being the single muon signal (1 VEM) too small to be detectable by the SPMT, the absolute scale in physical units is obtained by cross-calibrating the SPMT and LPMT signals in the overlapping region, as shown in Fig. 3 (red dots) for one of the AugerPrime engineering array stations. A dedicated trigger selecting small local showers is set up to this aim, furthermore imposing a minimum threshold of $\sim$80 VEM on the LPMTs to guarantee a reasonably large signal on the SPMT, not affected too much by statistical fluctuations. The distribution of Fig. 3 is then fitted in the region of superposition of the two PMTs (excluding the LPMT saturation) to obtain the slope, i.e. the calibration value to convert to VEM the integrated charge of the SPMT.

The SPMT gain is tuned by this automated procedure only during the first 24 hours following the installation; successively the value of the slope is continuously monitored and its value updated in the offline data analysis. Indeed a variation of the slope with the temperature is expected, as the temperature dependence of the gain is accounted for in the calibration of the LPMTs only.

The charge spectrum for a single station of AugerPrime is shown in Fig. 4, as measured by the standard LPMTs (blue histogram for the anode channel) and by the SPMT (red histogram for the unsaturated SPMT; in cyan, the few values where the SPMT is saturated too). The dynamic range is extended from $\sim10^3$ VEM to few $\sim10^4$ VEM obeying the power law behaviour expected for the distribution of the signal from individual stations.

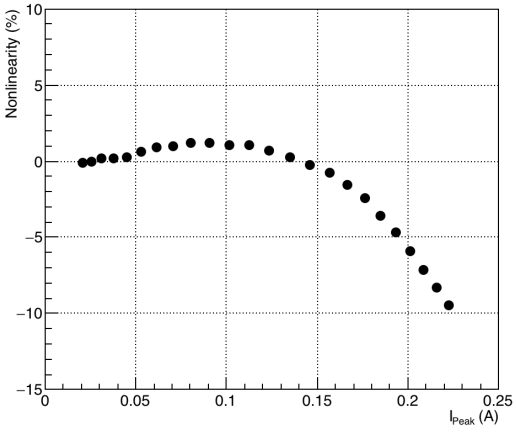

Figure 5: Linearity behaviour of one of the R9420 employed in the AugerPrime scintillators. The photomultiplier is linear within 5% up to ∼160 mA as required.

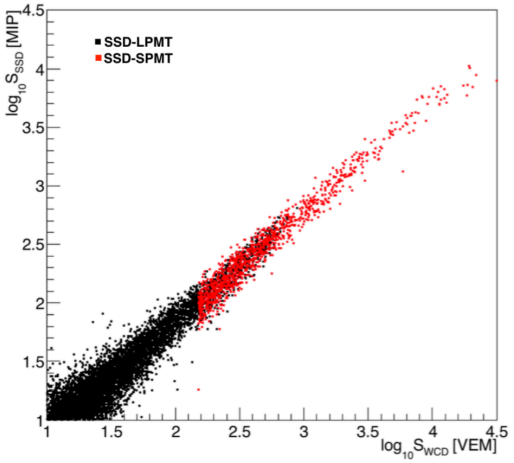

Figure 6: Relation between the water-Cherenkov station and the scintillator signals as measured by one detector of AugerPrime.

2.2 Extended dynamic range of the scintillator detectors

Each surface scintillator detector (SSD) consists of two identical modules made of extruded plastic scintillator bars, read by U-shaped 1.0 mm wavelength-shifting (WLS) fibers. A single photomultiplier is optically coupled to a bundle collecting the 48 fibers from both the modules and integrating the total signal of all bars. This configuration combines extreme simplicity with excellent performance/cost balance, giving both a satisfactory light yield of ∼30 phe/MIP (photoelectrons per minimum ionizing particle) and an acceptable spatial non uniformity (±10%).

Care is required in the choice of the best photomultiplier for this application, because of the requirement on the dynamic range. For consistency with the associated water-Cherenkov detector, it must in fact span from the signal of a single particle, as needed for calibration, to large signals, up to $\sim 2\times10^4$ MIP. The Hamamatsu R9420 photomultiplier (8 stage, 1.5 inch bialkali photocathode) has been chosen in the baseline design based on its excellent linear response also when operated at low gain. The tube is in fact linear within 5% for peak currents up to 160 mA (for a gain of 8×10^4), as shown in Fig. 5. In the electronics front-end, the R9420 anode signal is filtered and split in two in a similar way as the signals from the standard LPMTs of the surface stations. To reach the required dynamic range after the splitting, one of the two signals is attenuated by a factor of 4, while the other is amplified by a factor of 32 [3]. The SSD calibration is based on the signal deposited by a minimum ionising particle (MIP) crossing the detector. About 40% of the calibration triggers of the water-Cherenkov stations produces a corresponding MIP in the scintillator. The statistics of calibration events recorded in a minute, corresponding to the standard calibration interval for the water-Cherenkov detectors, is therefore enough to obtain a precise measurement of the MIP.

An example of the relation between the signals in one of the water-Cherenkov stations and in the corresponding scintillator is shown in Fig. 6, exploiting the recordings of 4 months of data taken by the engineering array of AugerPrime. Both scales are expressed in physical units: the SPMT response is calibrated in VEM and the scintillator photomultiplier in MIP as discussed before. The dynamic range in the surface detector is nicely covered by the LPMTs up to the saturation (black

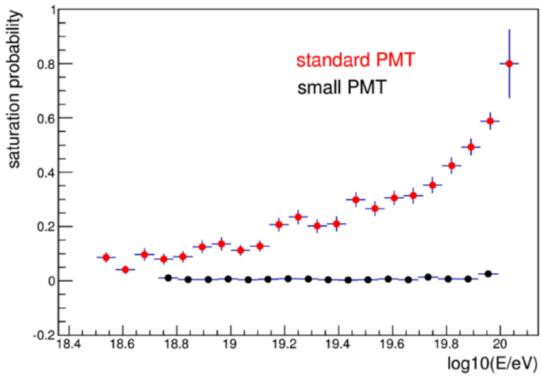

Figure 7: Probability of at least one saturated station/event as a function of energy.

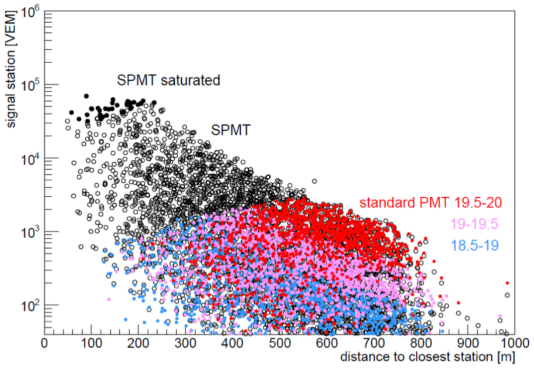

Figure 8: Simulated signals as a function of distance to shower core for different energies.

dots) and then extended to the highest particle densities by the SPMT (red dots) up to the highest particle densities measured by one detector of AugerPrime.

3. Expected physics performance

A large set of simulations of air showers induced by primary protons with energy between 3 and 100 EeV (based on the CORSIKA code [4]) has been generated to to demonstrate the benefits of the extended dynamic range.

The broadening of the dynamic range by more than a decade is highly expected to record an event above 10^{20} eV unambiguously, with full signals in all stations. Due to the limited dynamic range of the LPMTs and old electronics, the probability of having at least one saturated station (the closest to the shower core) per event was steadily increasing with energy, reaching ∼30% at $10^{19.5}$ eV, as shown in Fig. 7 (red dots). In AugerPrime, thanks to the SPMT installation, this probability is basically zero in the whole range (black dots).

As demonstrated above in Fig. 6, the dynamic range is increased by more than one decade in both the water-Cherenkov and the scintillator detectors, thus helping in unambiguously separating the shower components in all stations and to cross check the two measurements, which are affected by different systematic uncertainties.

A comparison of the signals measured at different distances to the shower core is shown in Fig. 8 for different energies in the case of the LPMTs (coloured circles) and of the SPMT (black circles) for the same air showers. Complete signals could be measured at the highest energies (above $10^{19.5}$ eV) only above ∼500 to 600 m from the shower core. With the increased dynamic range, we will be able to measure the lateral distribution function of the showers down to distances as close as 250 to 300 m from the shower core; below this distance, the uncertainty in the core position would anyway limit the usefulness of the measurements. We will thus be able to test the modelling of the lateral distribution function in a range of distances never before explored at these ultra high energies and to study the shower components in the region where most of the energy is deposited.

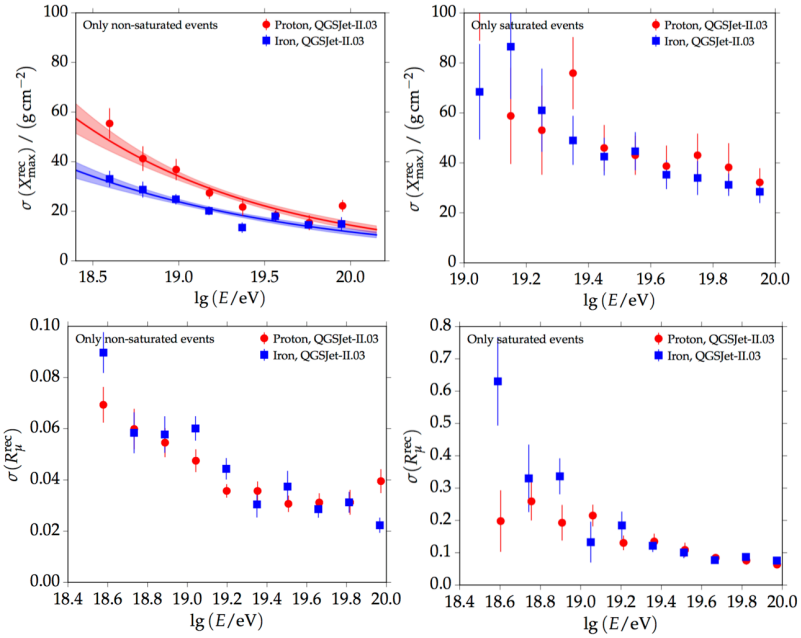

Figure 9: Resolution of the $X_{\rm max}$ (top panel) and of the relative number of muons R_μ (bottom panel) as obtained from universality, derived using non saturated (left) or saturated-only (right) events.

The signal variance in the extended dynamic range interval will be reduced significantly, being dominated by the calibration uncertainties (see Fig. 2). Event selection based on cuts in energy will be more accurate and flux corrections of the energy spectrum due to resolution-dependent migrations will be smaller.

The complementarity of the techniques employed in AugerPrime will allow us to efficiently separate the two main components of the air showers at the ground, namely the electromagnetic and the muonic ones. Exploiting the fact that the ratio between the two components is more than a factor two higher in the unshielded scintillator slab than in the water-Cherenkov detector, the muonic signal can be derived on a station-by-station basis. On the other hand, an analysis based on shower universality ([5] and references therein) allows us to correlate the detector signals at different lateral distances, taking also advantage of the temporal structure of the signal measured in the detectors. In the latter, a parametrization of the signals is expressed as a function of the air shower macro parameters, e.g. the depth of shower maximum $X_{\rm max}$ or the muon content relative to a reference model R_μ.

As shown in Fig.9, the universality method allows us to reconstruct an unbiased $X_{\rm max}$ with an energy dependent resolution of $\sim$50 g/cm^2 to $\sim$20 g/cm^2, with a spread smaller for iron induced showers as compared to proton induced ones, when using only non saturated events. The same conclusion can be drawn for R_μ: the resolution in the relative number of muons stays below 10% at all energies if saturation is cured.

An engineering array of 12 stations has been deployed in the field and has been taking data since few months [6]. In Fig. 10 we show the lateral distribution of one of the measured events, reconstructed with $E = 1.59\times10^{19}$ eV and arrival direction $\theta = 16^\circ$. For the station closest to the shower core (here at 153 m) both the saturated signal from the LPMTs and the full signal from the

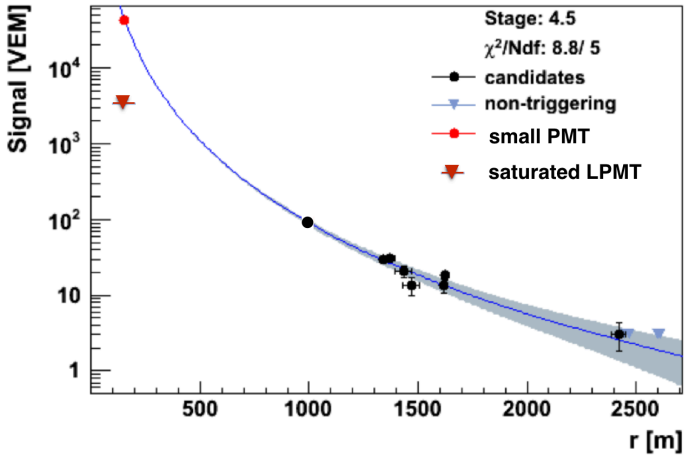

Figure 10: Lateral distribution for one event measured in the engineering array of AugerPrime. The signal in the station closest to the shower core (153 m) is recorded by the SPMT (red point); the signal in the LPMTs is saturated (red triangle).

SPMT are shown.

4. Summary

The dynamic range of the AugerPrime upgrade of the Pierre Auger Observatory has been extended to particle densities as high as few thousand per m^2, thus allowing us to measure full signals from all the stations of the air shower footprints at the ground down to a distance of about 250 m from the shower core.

A small diameter PMT has been added to this aim in the water-Cherenkov detectors, while a PMT with suitable range has been chosen for the scintillators. They have been deployed in the engineering array of AugerPrime and their data are now under scrutiny. The first results confirm the effectiveness of the choice and the expected behaviour of the measurements.

References

[1] D. Veberič (Pierre Auger Coll.), *Estimation of Signal in Saturated Stations of Pierre Auger Surface Detector*, Proc. 33rd Int. Cosmic Ray Conf., Rio de Janeiro, Brasil, arXiv:1307.5059.

[2] The Pierre Auger Collaboration, *The AugerPrime Design Report*, arXiv:1604.03637.

[3] T. Suomijarvi, for the Pierre Auger Collaboration, *The AugerPrime electronics*, these Proceedings.

[4] D. Heck, J. Knapp, J.N. Capdevielle *et al.*, *CORSIKA: a Monte Carlo code to simulate extensive air showers*, FZKA 6019 (Forschungszentrum, Karlsruhe, 1998).

[5] M. Ave, M. Roth, and A. Schulz, *A universal description of temporal and lateral distributions of ground particles in extensive air showers*, Proc. 34th Int. Cosmic Ray Conf., The Hague, Netherlands, PoS (2015) 378.

[6] Z. Zong, for the Pierre Auger Collaboration, *The first results from the AugerPrime Engineering Array*, these Proceedings.

The Pierre Auger Collaboration

A. Aab[77], P. Abreu[69], M. Aglietta[50,49], I.F.M. Albuquerque[18], I. Allekotte[1], A. Almela[8,11], J. Alvarez Castillo[65], J. Alvarez-Muñiz[76], G.A. Anastasi[41,43], L. Anchordoqui[83], B. Andrada[8], S. Andringa[69], C. Aramo[47], N. Arsene[71], H. Asorey[1,27], P. Assis[69], J. Aublin[32], G. Avila[9,10], A.M. Badescu[72], A. Balaceanu[70], F. Barbato[57], R.J. Barreira Luz[69], K.H. Becker[34], J.A. Bellido[12], C. Berat[33], M.E. Bertaina[59,49], X. Bertou[1], P.L. Biermann[b], J. Biteau[31], S.G. Blaess[12], A. Blanco[69], J. Blazek[29], C. Bleve[53,45], M. Boháčová[29], D. Boncioli[43,g], C. Bonifazi[24], N. Borodai[66], A.M. Botti[8,36], J. Brack[f], I. Brancus[70], T. Bretz[38], A. Bridgeman[35], F.L. Briechle[38], P. Buchholz[40], A. Bueno[75], S. Buitink[77], M. Buscemi[55,44], K.S. Caballero-Mora[63], B. Caccianiga[46], L. Caccianiga[56], A. Cancio[11,8], F. Canfora[77], L. Caramete[71], R. Caruso[55,44], A. Castellina[50,49], F. Catalani[16], G. Cataldi[45], L. Cazon[69], A.G. Chavez[64], J.A. Chinellato[19], J. Chudoba[29], R.W. Clay[12], A. Cobos[8], R. Colalillo[57,47], A. Coleman[87], L. Collica[49], M.R. Coluccia[53,45], R. Conceição[69], G. Consolati[46], G. Consolati[46,51], F. Contreras[9,10], M.J. Cooper[12], S. Coutu[87], C.E. Covault[81], J. Cronin[88], S. D'Amico[52,45], B. Daniel[19], S. Dasso[5,3], K. Daumiller[36], B.R. Dawson[12], R.M. de Almeida[26], S.J. de Jong[77,79], G. De Mauro[77], J.R.T. de Mello Neto[24,25], I. De Mitri[53,45], J. de Oliveira[26], V. de Souza[17], J. Debatin[35], O. Deligny[31], M.L. Díaz Castro[19], F. Diogo[69], C. Dobrigkeit[19], J.C. D'Olivo[65], Q. Dorosti[40], R.C. dos Anjos[23], M.T. Dova[4], A. Dundovic[39], J. Ebr[29], R. Engel[36], M. Erdmann[38], M. Erfani[40], C.O. Escobar[e], J. Espadanal[69], A. Etchegoyen[8,11], H. Falcke[77,80,79], J. Farmer[88], G. Farrar[85], A.C. Fauth[19], N. Fazzini[e], F. Fenu[59,49], B. Fick[84], J.M. Figueira[8], A. Filipčič[74,73], M.M. Freire[6], T. Fujii[88], A. Fuster[8,11], R. Gaïor[32], B. García[7], F. Gaté[d], H. Gemmeke[37], A. Gherghel-Lascu[70], U. Giaccari[24], M. Giammarchi[46], M. Giller[67], D. Głas[68], C. Glaser[38], G. Golup[1], M. Gómez Berisso[1], P.F. Gómez Vitale[9,10], N. González[8,36], A. Gorgi[50,49], A.F. Grillo[43], T.D. Grubb[12], F. Guarino[57,47], G.P. Guedes[20], R. Halliday[81], M.R. Hampel[8], P. Hansen[4], D. Harari[1], T.A. Harrison[12], A. Haungs[36], T. Hebbeker[38], D. Heck[36], P. Heimann[40], A.E. Herve[35], G.C. Hill[12], C. Hojvat[e], E. Holt[36,8], P. Homola[66], J.R. Hörandel[77,79], P. Horvath[30], M. Hrabovský[30], T. Huege[36], J. Hulsman[8,36], A. Insolia[55,44], P.G. Isar[71], I. Jandt[34], J.A. Johnsen[82], M. Josebachuili[8], J. Jurysek[29], A. Kääpä[34], O. Kambeitz[35], K.H. Kampert[34], B. Keilhauer[36], N. Kemmerich[18], E. Kemp[19], J. Kemp[38], R.M. Kieckhafer[84], H.O. Klages[36], M. Kleifges[37], J. Kleinfeller[9], R. Krause[38], N. Krohm[34], D. Kuempel[34], G. Kukec Mezek[73], N. Kunka[37], A. Kuotb Awad[35], B.L. Lago[15], D. LaHurd[81], R.G. Lang[17], M. Lauscher[38], R. Legumina[67], M.A. Leigui de Oliveira[22], A. Letessier-Selvon[32], I. Lhenry-Yvon[31], K. Link[35], D. Lo Presti[55], L. Lopes[69], R. López[60], A. López Casado[76], R. Lorek[81], Q. Luce[31], A. Lucero[8,11], M. Malacari[88], M. Mallamaci[56,46], D. Mandat[29], P. Mantsch[e], A.G. Mariazzi[4], I.C. Mariş[13], G. Marsella[53,45], D. Martello[53,45], H. Martinez[61], O. Martínez Bravo[60], J.J. Masías Meza[3], H.J. Mathes[36], S. Mathys[34], G. Matthiae[58,48], E. Mayotte[34], P.O. Mazur[e], C. Medina[82], G. Medina-Tanco[65], D. Melo[8], A. Menshikov[37], K.-D. Merenda[82], S. Michal[30], M.I. Micheletti[6], L. Middendorf[38], L. Miramonti[56,46], B. Mitrica[70], D. Mockler[35], S. Mollerach[1], F. Montanet[33], C. Morello[50,49], G. Morlino[41,43], M. Mostafá[87], A.L. Müller[8,36], G. Müller[38], M.A. Muller[19,21], S. Müller[35,8], R. Mussa[49], I. Naranjo[1], L. Nellen[65], P.H. Nguyen[12], M. Niculescu-Oglinzanu[70], M. Niechciol[40], L. Niemietz[34], T. Niggemann[38], D. Nitz[84], D. Nosek[28], V. Novotny[28], L. Nožka[30], L.A. Núñez[27], L. Ochilo[40], F. Oikonomou[87], A. Olinto[88], M. Palatka[29], J. Pallotta[2], P. Papenbreer[34], G. Parente[76], A. Parra[60], T. Paul[83], M. Pech[29], F. Pedreira[76], J. Pękala[66], R. Pelayo[62], J. Peña-Rodriguez[27], L. A. S. Pereira[19], M. Perlin[8], L. Perrone[53,45], C. Peters[38], S. Petrera[41,43], J. Phuntsok[87], R. Piegaia[3], T. Pierog[36], M. Pimenta[69], V. Pirronello[55,44], M. Platino[8], M. Plum[38], J. Poh[88], C. Porowski[66], R.R. Prado[17], P. Privitera[88], M. Prouza[29], E.J. Quel[2], S. Querchfeld[34], S. Quinn[81], R. Ramos-Pollan[27], J. Rautenberg[34], D. Ravignani[8], J. Ridky[29], F. Riehn[69], M. Risse[40], P. Ristori[2], V. Rizi[54,43], W. Rodrigues de Carvalho[18], G. Rodriguez Fernandez[58,48], J. Rodriguez Rojo[9], M.J. Roncoroni[8], M. Roth[36], E. Roulet[1], A.C. Rovero[5], P. Ruehl[40], S.J. Saffi[12], A. Saftoiu[70],

F. Salamida[54,43], H. Salazar[60], A. Saleh[73], G. Salina[48], F. Sánchez[8], P. Sanchez-Lucas[75], E.M. Santos[18], E. Santos[8], F. Sarazin[82], R. Sarmento[69], C. Sarmiento-Cano[8], R. Sato[9], M. Schauer[34], V. Scherini[45], H. Schieler[36], M. Schimp[34], D. Schmidt[36,8], O. Scholten[78,c], P. Schovánek[29], F.G. Schröder[36], S. Schröder[34], A. Schulz[35], J. Schumacher[38], S.J. Sciutto[4], A. Segreto[42,44], R.C. Shellard[14], G. Sigl[39], G. Silli[8,36], R. Šmída[36], G.R. Snow[89], P. Sommers[87], S. Sonntag[40], J. F. Soriano[83], R. Squartini[9], D. Stanca[70], S. Stanič[73], J. Stasielak[66], P. Stassi[33], M. Stolpovskiy[33], F. Strafella[53,45], A. Streich[35], F. Suarez[8,11], M. Suarez Durán[27], T. Sudholz[12], T. Suomijärvi[31], A.D. Supanitsky[5], J. Šupík[30], J. Swain[86], Z. Szadkowski[68], A. Taboada[36], O.A. Taborda[1], V.M. Theodoro[19], C. Timmermans[79,77], C.J. Todero Peixoto[16], L. Tomankova[36], B. Tomé[69], G. Torralba Elipe[76], P. Travnicek[29], M. Trini[73], R. Ulrich[36], M. Unger[36], M. Urban[38], J.F. Valdés Galicia[65], I. Valiño[76], L. Valore[57,47], G. van Aar[77], P. van Bodegom[12], A.M. van den Berg[78], A. van Vliet[77], E. Varela[60], B. Vargas Cárdenas[65], R.A. Vázquez[76], D. Veberič[36], C. Ventura[25], I.D. Vergara Quispe[4], V. Verzi[48], J. Vicha[29], L. Villaseñor[64], S. Vorobiov[73], H. Wahlberg[4], O. Wainberg[8,11], D. Walz[38], A.A. Watson[a], M. Weber[37], A. Weindl[36], M. Wiedeński[68], L. Wiencke[82], H. Wilczyński[66], T. Winchen[34], M. Wirtz[38], D. Wittkowski[34], B. Wundheiler[8], L. Yang[73], A. Yushkov[8], E. Zas[76], D. Zavrtanik[73,74], M. Zavrtanik[74,73], A. Zepeda[61], B. Zimmermann[37], M. Ziolkowski[40], Z. Zong[31], F. Zuccarello[55,44]

—•—

[1] Centro Atómico Bariloche and Instituto Balseiro (CNEA-UNCuyo-CONICET), San Carlos de Bariloche, Argentina
[2] Centro de Investigaciones en Láseres y Aplicaciones, CITEDEF and CONICET, Villa Martelli, Argentina
[3] Departamento de Física and Departamento de Ciencias de la Atmósfera y los Océanos, FCEyN, Universidad de Buenos Aires and CONICET, Buenos Aires, Argentina
[4] IFLP, Universidad Nacional de La Plata and CONICET, La Plata, Argentina
[5] Instituto de Astronomía y Física del Espacio (IAFE, CONICET-UBA), Buenos Aires, Argentina
[6] Instituto de Física de Rosario (IFIR) - CONICET/U.N.R. and Facultad de Ciencias Bioquímicas y Farmacéuticas U.N.R., Rosario, Argentina
[7] Instituto de Tecnologías en Detección y Astropartículas (CNEA, CONICET, UNSAM), and Universidad Tecnológica Nacional - Facultad Regional Mendoza (CONICET/CNEA), Mendoza, Argentina
[8] Instituto de Tecnologías en Detección y Astropartículas (CNEA, CONICET, UNSAM), Buenos Aires, Argentina
[9] Observatorio Pierre Auger, Malargüe, Argentina
[10] Observatorio Pierre Auger and Comisión Nacional de Energía Atómica, Malargüe, Argentina
[11] Universidad Tecnológica Nacional - Facultad Regional Buenos Aires, Buenos Aires, Argentina
[12] University of Adelaide, Adelaide, S.A., Australia
[13] Université Libre de Bruxelles (ULB), Brussels, Belgium
[14] Centro Brasileiro de Pesquisas Fisicas, Rio de Janeiro, RJ, Brazil
[15] Centro Federal de Educação Tecnológica Celso Suckow da Fonseca, Nova Friburgo, Brazil
[16] Universidade de São Paulo, Escola de Engenharia de Lorena, Lorena, SP, Brazil
[17] Universidade de São Paulo, Instituto de Física de São Carlos, São Carlos, SP, Brazil
[18] Universidade de São Paulo, Instituto de Física, São Paulo, SP, Brazil
[19] Universidade Estadual de Campinas, IFGW, Campinas, SP, Brazil
[20] Universidade Estadual de Feira de Santana, Feira de Santana, Brazil
[21] Universidade Federal de Pelotas, Pelotas, RS, Brazil
[22] Universidade Federal do ABC, Santo André, SP, Brazil
[23] Universidade Federal do Paraná, Setor Palotina, Palotina, Brazil
[24] Universidade Federal do Rio de Janeiro, Instituto de Física, Rio de Janeiro, RJ, Brazil
[25] Universidade Federal do Rio de Janeiro (UFRJ), Observatório do Valongo, Rio de Janeiro, RJ, Brazil

[26] Universidade Federal Fluminense, EEIMVR, Volta Redonda, RJ, Brazil
[27] Universidad Industrial de Santander, Bucaramanga, Colombia
[28] Charles University, Faculty of Mathematics and Physics, Institute of Particle and Nuclear Physics, Prague, Czech Republic
[29] Institute of Physics of the Czech Academy of Sciences, Prague, Czech Republic
[30] Palacky University, RCPTM, Olomouc, Czech Republic
[31] Institut de Physique Nucléaire d'Orsay (IPNO), Université Paris-Sud, Univ. Paris/Saclay, CNRS-IN2P3, Orsay, France
[32] Laboratoire de Physique Nucléaire et de Hautes Energies (LPNHE), Universités Paris 6 et Paris 7, CNRS-IN2P3, Paris, France
[33] Laboratoire de Physique Subatomique et de Cosmologie (LPSC), Université Grenoble-Alpes, CNRS/IN2P3, Grenoble, France
[34] Bergische Universität Wuppertal, Department of Physics, Wuppertal, Germany
[35] Karlsruhe Institute of Technology, Institut für Experimentelle Kernphysik (IEKP), Karlsruhe, Germany
[36] Karlsruhe Institute of Technology, Institut für Kernphysik, Karlsruhe, Germany
[37] Karlsruhe Institute of Technology, Institut für Prozessdatenverarbeitung und Elektronik, Karlsruhe, Germany
[38] RWTH Aachen University, III. Physikalisches Institut A, Aachen, Germany
[39] Universität Hamburg, II. Institut für Theoretische Physik, Hamburg, Germany
[40] Universität Siegen, Fachbereich 7 Physik - Experimentelle Teilchenphysik, Siegen, Germany
[41] Gran Sasso Science Institute (INFN), L'Aquila, Italy
[42] INAF - Istituto di Astrofisica Spaziale e Fisica Cosmica di Palermo, Palermo, Italy
[43] INFN Laboratori Nazionali del Gran Sasso, Assergi (L'Aquila), Italy
[44] INFN, Sezione di Catania, Catania, Italy
[45] INFN, Sezione di Lecce, Lecce, Italy
[46] INFN, Sezione di Milano, Milano, Italy
[47] INFN, Sezione di Napoli, Napoli, Italy
[48] INFN, Sezione di Roma "Tor Vergata", Roma, Italy
[49] INFN, Sezione di Torino, Torino, Italy
[50] Osservatorio Astrofisico di Torino (INAF), Torino, Italy
[51] Politecnico di Milano, Dipartimento di Scienze e Tecnologie Aerospaziali , Milano, Italy
[52] Università del Salento, Dipartimento di Ingegneria, Lecce, Italy
[53] Università del Salento, Dipartimento di Matematica e Fisica “E. De Giorgi”, Lecce, Italy
[54] Università dell'Aquila, Dipartimento di Scienze Fisiche e Chimiche, L'Aquila, Italy
[55] Università di Catania, Dipartimento di Fisica e Astronomia, Catania, Italy
[56] Università di Milano, Dipartimento di Fisica, Milano, Italy
[57] Università di Napoli "Federico II", Dipartimento di Fisica “Ettore Pancini“, Napoli, Italy
[58] Università di Roma “Tor Vergata”, Dipartimento di Fisica, Roma, Italy
[59] Università Torino, Dipartimento di Fisica, Torino, Italy
[60] Benemérita Universidad Autónoma de Puebla, Puebla, México
[61] Centro de Investigación y de Estudios Avanzados del IPN (CINVESTAV), México, D.F., México
[62] Unidad Profesional Interdisciplinaria en Ingeniería y Tecnologías Avanzadas del Instituto Politécnico Nacional (UPIITA-IPN), México, D.F., México
[63] Universidad Autónoma de Chiapas, Tuxtla Gutiérrez, Chiapas, México
[64] Universidad Michoacana de San Nicolás de Hidalgo, Morelia, Michoacán, México
[65] Universidad Nacional Autónoma de México, México, D.F., México
[66] Institute of Nuclear Physics PAN, Krakow, Poland
[67] University of Łódź, Faculty of Astrophysics, Łódź, Poland

[68] University of Łódź, Faculty of High-Energy Astrophysics,Łódź, Poland
[69] Laboratório de Instrumentação e Física Experimental de Partículas - LIP and Instituto Superior Técnico - IST, Universidade de Lisboa - UL, Lisboa, Portugal
[70] "Horia Hulubei" National Institute for Physics and Nuclear Engineering, Bucharest-Magurele, Romania
[71] Institute of Space Science, Bucharest-Magurele, Romania
[72] University Politehnica of Bucharest, Bucharest, Romania
[73] Center for Astrophysics and Cosmology (CAC), University of Nova Gorica, Nova Gorica, Slovenia
[74] Experimental Particle Physics Department, J. Stefan Institute, Ljubljana, Slovenia
[75] Universidad de Granada and C.A.F.P.E., Granada, Spain
[76] Universidad de Santiago de Compostela, Santiago de Compostela, Spain
[77] IMAPP, Radboud University Nijmegen, Nijmegen, The Netherlands
[78] KVI - Center for Advanced Radiation Technology, University of Groningen, Groningen, The Netherlands
[79] Nationaal Instituut voor Kernfysica en Hoge Energie Fysica (NIKHEF), Science Park, Amsterdam, The Netherlands
[80] Stichting Astronomisch Onderzoek in Nederland (ASTRON), Dwingeloo, The Netherlands
[81] Case Western Reserve University, Cleveland, OH, USA
[82] Colorado School of Mines, Golden, CO, USA
[83] Department of Physics and Astronomy, Lehman College, City University of New York, Bronx, NY, USA
[84] Michigan Technological University, Houghton, MI, USA
[85] New York University, New York, NY, USA
[86] Northeastern University, Boston, MA, USA
[87] Pennsylvania State University, University Park, PA, USA
[88] University of Chicago, Enrico Fermi Institute, Chicago, IL, USA
[89] University of Nebraska, Lincoln, NE, USA

———

[a] School of Physics and Astronomy, University of Leeds, Leeds, United Kingdom
[b] Max-Planck-Institut für Radioastronomie, Bonn, Germany
[c] also at Vrije Universiteit Brussels, Brussels, Belgium
[d] SUBATECH, École des Mines de Nantes, CNRS-IN2P3, Université de Nantes, France
[e] Fermi National Accelerator Laboratory, USA
[f] Colorado State University, Fort Collins, CO
[g] now at Deutsches Elektronen-Synchrotron (DESY), Zeuthen, Germany

Acknowledgments

The successful installation, commissioning, and operation of the Pierre Auger Observatory would not have been possible without the strong commitment and effort from the technical and administrative staff in Malargüe. We are very grateful to the following agencies and organizations for financial support:

Argentina – Comisión Nacional de Energía Atómica; Agencia Nacional de Promoción Científica y Tecnológica (ANPCyT); Consejo Nacional de Investigaciones Científicas y Técnicas (CONICET); Gobierno de la Provincia de Mendoza; Municipalidad de Malargüe; NDM Holdings and Valle Las Leñas; in gratitude for their continuing cooperation over land access; Australia – the Australian Research Council; Brazil – Conselho Nacional de Desenvolvimento Científico e Tecnológico (CNPq); Financiadora de Estudos e Projetos (FINEP); Fundação de Amparo à Pesquisa do Estado de Rio de Janeiro (FAPERJ); São Paulo Research Foundation (FAPESP) Grants No. 2010/07359-6 and No. 1999/05404-3; Ministério de Ciência e Tecnologia (MCT); Czech Republic – Grant No. MSMT CR LG15014, LO1305, LM2015038 and CZ.02.1.01/0.0/0.0/16_013/0001402; France – Centre de Calcul IN2P3/CNRS; Centre National de la Recherche Scientifique (CNRS); Conseil Régional Ile-de-France; Département Physique Nucléaire et Corpusculaire (PNC-IN2P3/CNRS); Département Sciences de l'Univers (SDU-INSU/CNRS); Institut Lagrange de Paris (ILP) Grant No. LABEX ANR-10-LABX-63 within the Investissements d'Avenir

Programme Grant No. ANR-11-IDEX-0004-02; Germany – Bundesministerium für Bildung und Forschung (BMBF); Deutsche Forschungsgemeinschaft (DFG); Finanzministerium Baden-Württemberg; Helmholtz Alliance for Astroparticle Physics (HAP); Helmholtz-Gemeinschaft Deutscher Forschungszentren (HGF); Ministerium für Innovation, Wissenschaft und Forschung des Landes Nordrhein-Westfalen; Ministerium für Wissenschaft, Forschung und Kunst des Landes Baden-Württemberg; Italy – Istituto Nazionale di Fisica Nucleare (INFN); Istituto Nazionale di Astrofisica (INAF); Ministero dell'Istruzione, dell'Universitá e della Ricerca (MIUR); CETEMPS Center of Excellence; Ministero degli Affari Esteri (MAE); Mexico – Consejo Nacional de Ciencia y Tecnología (CONACYT) No. 167733; Universidad Nacional Autónoma de México (UNAM); PAPIIT DGAPA-UNAM; The Netherlands – Ministerie van Onderwijs, Cultuur en Wetenschap; Nederlandse Organisatie voor Wetenschappelijk Onderzoek (NWO); Stichting voor Fundamenteel Onderzoek der Materie (FOM); Poland – National Centre for Research and Development, Grants No. ERA-NET-ASPERA/01/11 and No. ERA-NET-ASPERA/02/11; National Science Centre, Grants No. 2013/08/M/ST9/00322, No. 2013/08/M/ST9/00728 and No. HARMONIA 5–2013/10/M/ST9/00062, UMO-2016/22/M/ST9/00198; Portugal – Portuguese national funds and FEDER funds within Programa Operacional Factores de Competitividade through Fundação para a Ciência e a Tecnologia (COMPETE); Romania – Romanian Authority for Scientific Research ANCS; CNDI-UEFISCDI partnership projects Grants No. 20/2012 and No. 194/2012 and PN 16 42 01 02; Slovenia – Slovenian Research Agency; Spain – Comunidad de Madrid; Fondo Europeo de Desarrollo Regional (FEDER) funds; Ministerio de Economía y Competitividad; Xunta de Galicia; European Community 7th Framework Program Grant No. FP7-PEOPLE-2012-IEF-328826; USA – Department of Energy, Contracts No. DE-AC02-07CH11359, No. DE-FR02-04ER41300, No. DE-FG02-99ER41107 and No. DE-SC0011689; National Science Foundation, Grant No. 0450696; The Grainger Foundation; Marie Curie-IRSES/EPLANET; European Particle Physics Latin American Network; European Union 7th Framework Program, Grant No. PIRSES-2009-GA-246806; European Union's Horizon 2020 research and innovation programme (Grant No. 646623); and UNESCO.

Last modified on 2017-07-31.